

Quantitative study of the stabilization parameter in the virtual element method

Alessandro Russo^{1,2} and N. Sukumar³

¹ University of Milano-Bicocca, 20133 Milano, Italy,

² IMATI-CNR, 27100 Pavia, Italy

alessandro.russo@unimib.it

³ University of California, Davis CA 95616, USA

nsukumar@ucdavis.edu

Abstract. The choice of stabilization term is a critical component of the virtual element method (VEM). However, the theory of VEM provides only asymptotic guidance for selecting the stabilization term, which ensures convergence as the mesh size approaches zero, but does not provide a unique prescription for its exact form. Thus, the selection of a suitable stabilization term is often guided by numerical experimentation and analysis of the resulting solution, including factors such as stability, accuracy, and efficiency. In this paper, we establish a new link between VEM and generalized barycentric coordinates, in particular isoparametric finite elements as a specific case. This connection enables the interpretation of the stability as the energy of a particular function in the discrete space, commonly known as the ‘hourglass mode.’ Through this approach, this study sheds light on how the virtual element solution depends on the stabilization term, providing insights into the behavior of the method in more general scenarios.

Keywords: generalized barycentric coordinates, finite element method, virtual element method, hourglass modes, stabilization

1 Introduction

The virtual element method (VEM) [1,2] is a stabilized Galerkin method that is accurate and robust on polygonal and polyhedral meshes. The first-order VEM on simplices is identical to linear finite elements. Polygonal finite elements (see [3]) are based on generalized barycentric coordinates such as Wachspress basis (shape) functions [4] and mean value coordinates [5,6]. On a quadrilateral, isoparametric finite element shape functions are also an instance of GBCs.

In this paper, we present new results over the quadrilateral that provide clearer connections of the finite element method (FEM) and polygonal FEM to the virtual element method. A stabilization parameter is needed to ensure that the stiffness matrix in the VEM is consistent and stable (invertible). As noted in [7], this mirrors the development of hourglass finite elements over the four-node quadrilateral [8,9]. We first show that the stiffness matrix for the diffusion

equation on any (convex or nonconvex) quadrilateral can be written as the sum of two contributions: a consistency matrix \mathbf{A} that is exactly computable and a stabilization matrix that has the form $\tau\mathbf{B}$, where \mathbf{B} is known and the scalar τ is in fact the hourglass function associated with the shape functions of the four-node quadrilateral [7] (see Section 2). In Section 3, we compute values for τ on the square and parallelogram for isoparametric FEM and Wachspress shape functions. The decomposition of the element stiffness matrix in the VEM is precisely of the form $\mathbf{A} + \tau\mathbf{B}$, where τ is set to 1, which is elaborated in Section 4. We present two numerical examples in Section 5, and show that the standard value of τ in the VEM leads to a convergent scheme for the diffusion equation.

2 GBCs on a quadrilateral for the diffusion equation

Let Q be a quadrilateral with vertices $V_i = (x_i, y_i)$, $i = 1, 2, 3, 4$, and let $\{\varphi_i\}_{i=1}^4$ be a set of generalized barycentric coordinates such as isoparametric bilinear FEM, harmonic, Wachspress or mean value coordinates. Let κ be a constant

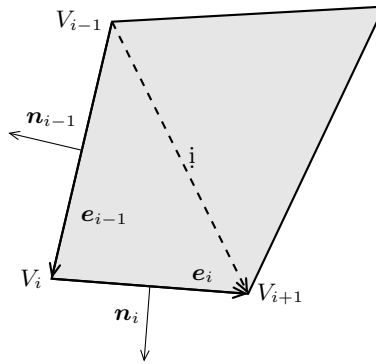


Fig. 1: The quadrilateral Q .

symmetric positive-definite 2×2 matrix on the element Q . Then the element stiffness matrix for the diffusion operator is defined by

$$\mathbf{K}_{ij} := \int_Q \kappa \nabla \varphi_j \cdot \nabla \varphi_i \, d\mathbf{x}. \quad (1)$$

We will prove the following structure theorem:

Theorem 1. *The matrix \mathbf{K} can be written as*

$$\mathbf{K} = \mathbf{A} + \tau\mathbf{B}, \quad (2)$$

where

- \mathbf{A} is a 4×4 matrix that depends only on the geometry of the quadrilateral Q and on the diffusion matrix $\boldsymbol{\kappa}$;
- \mathbf{B} is a 4×4 matrix that depend only on the geometry of the quadrilateral Q ; furthermore, \mathbf{B} is the same matrix for all parallelograms;
- τ is the energy of the function Ψ_h of our local space whose value at vertex V_i is $\frac{(-1)^i}{2}$, and is defined by

$$\tau := \int_Q \boldsymbol{\kappa} \nabla \Psi_h \cdot \nabla \Psi_h \, d\mathbf{x}. \quad (3)$$

Note that

$$\Psi_h = \frac{1}{2} (-\varphi_1 + \varphi_2 - \varphi_3 + \varphi_4). \quad (4)$$

The function Ψ_h is an hourglass mode (see [7]). The coefficient τ is the only term in (2) that depends on the explicit form of the basis functions.

Proof. Let Π_0^0 be the L^2 projection onto constants:

$$\Pi_0^0 w := \frac{1}{|Q|} \int_Q w \, d\mathbf{x}.$$

When the argument is a vector, Π_0^0 is applied componentwise. We start from the identity

$$\int_Q \boldsymbol{\kappa} \nabla u \cdot \nabla v \, d\mathbf{x} = \int_Q \boldsymbol{\kappa} \Pi_0^0 \nabla u \cdot \Pi_0^0 \nabla v \, d\mathbf{x} + \int_Q \boldsymbol{\kappa} (\mathbf{I} - \Pi_0^0) \nabla u \cdot (\mathbf{I} - \Pi_0^0) \nabla v \, d\mathbf{x}, \quad (5)$$

which holds true for $u, v \in H^1(P)$ (recall that $\boldsymbol{\kappa}$ is constant on Q).

2.1 The matrix \mathbf{A}

The matrix \mathbf{A} of (2) is simply given by the first term of (5) with $u = \varphi_j$, $v = \varphi_i$:

$$A_{ij} = \int_Q \boldsymbol{\kappa} \Pi_0^0 \nabla \varphi_j \cdot \Pi_0^0 \nabla \varphi_i \, d\mathbf{x} = \frac{1}{|Q|} \boldsymbol{\kappa} \left[\int_Q \nabla \varphi_j \, d\mathbf{x} \right] \cdot \left[\int_Q \nabla \varphi_i \, d\mathbf{x} \right].$$

Observe that A_{ij} is readily computable and does not depend on the explicit form of the basis functions, since by Gauss's formula

$$\int_Q \nabla \varphi_i \, d\mathbf{x} = \int_{\partial Q} \varphi_i \mathbf{n} \, ds = \frac{1}{2} \mathbf{d}_i^\perp, \quad (6)$$

where \mathbf{i} is the vector joining V_{i-1} with V_{i+1} (a diagonal of the quadrilateral, see Fig. 1) and \perp denotes clockwise rotation of 90° . Hence,

$$A_{ij} = \frac{1}{4|Q|} \boldsymbol{\kappa} \mathbf{d}_j^\perp \cdot \mathbf{d}_i^\perp. \quad (7)$$

Since in a quadrilateral we have $\mathfrak{3} = -1$ and $\mathfrak{4} = -2$, the matrix \mathbf{A} has a nice block structure:

$$\mathbf{A} = \begin{bmatrix} +\mathbf{C} & -\mathbf{C} \\ -\mathbf{C} & +\mathbf{C} \end{bmatrix} \quad \text{with} \quad \mathbf{C} := \begin{bmatrix} \kappa \mathbf{d}_1^\perp \cdot \mathbf{d}_1^\perp & \kappa \mathbf{d}_1^\perp \cdot \mathbf{d}_2^\perp \\ \kappa \mathbf{d}_1^\perp \cdot \mathbf{d}_2^\perp & \kappa \mathbf{d}_2^\perp \cdot \mathbf{d}_2^\perp \end{bmatrix}.$$

Remark 1. Note that if $\kappa = \kappa \mathbf{I}$, then we can remove the rotation:

$$A_{ij} = \frac{1}{4|Q|} \kappa_{\mathfrak{j}} \cdot \mathfrak{i}.$$

2.2 The matrix \mathbf{B}

Now we turn our attention to the second term of (5). The key idea is to write

$$\Pi_0^0 \nabla w \quad \text{as} \quad \nabla \Pi_1^\nabla w,$$

where $\Pi_1^\nabla w$ is a projection of w onto linear polynomials. More precisely, given any function v_h in our local space (i.e., a linear combination of the basis functions φ_i) we want to define a projection $\Pi_1^\nabla v_h$ onto linear polynomials such that:

- the gradient of $\Pi_1^\nabla v_h$ is the L^2 projection of the gradient of v_h , i.e.,

$$\nabla \Pi_1^\nabla v_h = \Pi_0^0 \nabla v_h = \frac{1}{|Q|} \int_Q \nabla v_h \, d\mathbf{x}; \quad (8)$$

- $\Pi_1^\nabla v_h$ depends only on the value of v_h on the boundary of Q (hence it is the same for all generalized barycentric coordinates).

We start by noting that (8) defines the value of the gradient of $\Pi_1^\nabla v_h$, and so it determines $\Pi_1^\nabla v_h$ up to a constant:

$$\Pi_1^\nabla v_h = \left(\frac{1}{|Q|} \int_Q \nabla v_h \, d\mathbf{x} \right) \cdot \mathbf{x} + \tilde{P}_0 v_h, \quad (9)$$

where \tilde{P}_0 is a projection onto constant functions to be fixed. Now we impose that Π_1^∇ is a projection onto linear polynomials, i.e.,

$$\text{if } \ell(\mathbf{x}) := \mathbf{a} \cdot \mathbf{x} + b \quad \text{then} \quad \Pi_1^\nabla \ell = \ell.$$

Since $\nabla \ell = \mathbf{a}$, we have

$$\Pi_1^\nabla \ell = \mathbf{a} \cdot \mathbf{x} + \tilde{P}_0 \ell = \mathbf{a} \cdot \mathbf{x} + \tilde{P}_0(\mathbf{a} \cdot \mathbf{x} + b) = \mathbf{a} \cdot \mathbf{x} + \tilde{P}_0(\mathbf{a} \cdot \mathbf{x}) + b = \ell + \mathbf{a} \cdot \tilde{P}_0 \mathbf{x}.$$

Hence the projection \tilde{P}_0 must satisfy

$$\tilde{P}_0 \mathbf{x} = 0, \quad \text{i.e.,} \quad \tilde{P}_0 x = 0 \quad \text{and} \quad \tilde{P}_0 y = 0.$$

A way to impose this condition is to start from an arbitrary projection onto constants, say P_0 , and then define

$$\tilde{P}_0 v_h := P_0 v_h - \left(\frac{1}{|Q|} \int_Q \nabla v_h \, d\mathbf{x} \right) \cdot P_0 \mathbf{x}. \quad (10)$$

We end up with the explicit formula

$$\Pi_1^\nabla v_h = \left(\frac{1}{|Q|} \int_Q \nabla v_h \, d\mathbf{x} \right) \cdot (\mathbf{x} - P_0 \mathbf{x}) + P_0 v_h, \quad (11)$$

where P_0 is an arbitrary projection onto constants.

Remark 2. An alternative way to define \tilde{P}_0 from P_0 is to start from (9) and impose the condition

$$P_0(\Pi_1^\nabla v_h - v_h) = 0.$$

In fact, from (9) we have

$$\begin{aligned} P_0(\Pi_1^\nabla v_h) &= \left(\frac{1}{|Q|} \int_Q \nabla v_h \, d\mathbf{x} \right) \cdot P_0 \mathbf{x} + P_0 \tilde{P}_0 v_h \\ &= \left(\frac{1}{|Q|} \int_Q \nabla v_h \, d\mathbf{x} \right) \cdot P_0 \mathbf{x} + \tilde{P}_0 v_h = P_0 v_h \end{aligned}$$

from which we get (10).

In order to be able to compute $\Pi_1^\nabla v_h$ without actually knowing v_h in the interior of P , the projector $P_0 v_h$ must be computable from the boundary values of v_h only. The two most natural choices are:

- $P_0 v_h := \frac{1}{N_P} \sum_{i=1}^4 v_h(V_i)$ (mean on the vertices of Q).

We have

$$P_0 \mathbf{x} = \frac{1}{4} \sum_{i=1}^4 V_i =: \bar{V} \quad (\text{vertex center}).$$

On taking $v_h = \varphi_i$, recalling (6) and observing that

$$P_0 \varphi_i = \frac{1}{4},$$

we have

$$\Pi_1^\nabla \varphi_i = \frac{1}{2|Q|} (\mathbf{x} - \bar{V}) \cdot \mathbf{d}_i^\perp + \frac{1}{4}. \quad (12)$$

- $P_0 v_h = \frac{1}{|\partial Q|} \int_{\partial Q} v_h \, ds$ (mean on the boundary of Q).

We have

$$P_0 \mathbf{x} = \frac{1}{|\partial Q|} \sum_{i=1}^4 \frac{V_i + V_{i+1}}{2} |\mathbf{e}_i| = \frac{1}{|\partial Q|} \sum_{i=1}^4 \frac{|\mathbf{e}_{i-1}| + |\mathbf{e}_i|}{2} V_i =: \tilde{V}.$$

On taking $v_h = \varphi_i$, recalling (6) and observing that

$$P_0\varphi_i = \frac{1}{|\partial P|} \frac{|\mathbf{e}_{i-1}| + |\mathbf{e}_i|}{2},$$

we have

$$\Pi_1^\nabla \varphi_i = \frac{1}{2|P|} (\mathbf{x} - \tilde{V}) \cdot \mathbf{d}_i^\perp + \frac{1}{|\partial P|} \frac{|\mathbf{e}_{i-1}| + |\mathbf{e}_i|}{2}. \quad (13)$$

It is clear that if all edges have the same length the two definitions of P_0 coincide. In what follows, we will assume that P_0 is defined either by (12) or by (13).

Remark 3. Observe that we cannot take as $P_0 v_h$ the mean value of v_h on Q , because we want that $\Pi_1^\nabla v_h$ depends only on the boundary value of v_h and not on its actual variation inside Q .

We now show that the function Ψ_h defined in (4) is in the kernel of Π_1^∇ ; actually, it turns out that $\ker \Pi_1^\nabla = \text{span} \{\Psi_h\}$. Recall that the function Ψ_h is defined as the (unique) function in our local space such that $\Psi_h(V_i) = \frac{(-1)^i}{2}$. We observe that Ψ_h has zero mean value on each edge, and hence

$$\int_Q \nabla \Psi_h \, d\mathbf{x} = \int_{\partial Q} \Psi_h \mathbf{n} \, ds = \sum_{i=1}^4 \left[\int_{\mathbf{e}_i} \Psi_h \, ds \right] \mathbf{n}_i = 0.$$

Furthermore, $P_0(\Psi_h) = 0$ for any of the two choices of P_0 given above. Hence, from (11), we have $\Pi_1^\nabla \Psi_h = 0$.

The function Ψ_h is linearly independent of the standard first-degree monomials $\{1, x, y\}$; hence the four functions $\{1, x, y, \Psi_h\}$ are a basis for our local space so that in particular any φ_i can be written as a linear combination of $1, x, y, \Psi_h$. To find the coefficients, we exploit the fact that the φ_i are generalized barycentric coordinates, that is

$$\sum_{i=1}^4 \varphi_i = 1, \quad \sum_{i=1}^4 x_i \varphi_i = x, \quad \sum_{i=1}^4 y_i \varphi_i = y$$

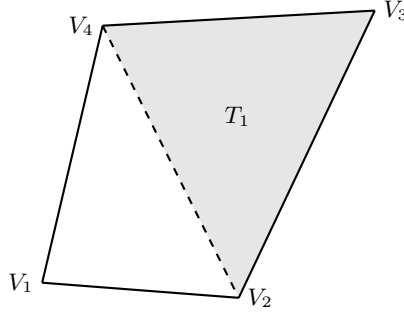
plus the equation defining Ψ_h :

$$\Psi_h = \frac{1}{2} (-\varphi_1 + \varphi_2 - \varphi_3 + \varphi_4).$$

In matrix form, we have

$$\begin{bmatrix} 1 & 1 & 1 & 1 \\ x_1 & x_2 & x_3 & x_4 \\ y_1 & y_2 & y_3 & y_4 \\ -\frac{1}{2} & \frac{1}{2} & -\frac{1}{2} & \frac{1}{2} \end{bmatrix} \begin{bmatrix} \varphi_1 \\ \varphi_2 \\ \varphi_3 \\ \varphi_4 \end{bmatrix} = \begin{bmatrix} 1 \\ x \\ y \\ \Psi_h \end{bmatrix}. \quad (14)$$

Let us denote by T_i the signed area of the triangle obtained by removing the vertex V_i from the quadrilateral Q and joining vertex V_{i-1} with vertex V_{i+1} (see Fig. 2). Therefore,


 Fig. 2: Signed area T_1 .

$$T_1 = \frac{1}{2} \det \begin{bmatrix} 1 & 1 & 1 \\ x_2 & x_3 & x_4 \\ y_2 & y_3 & y_4 \end{bmatrix}, \quad T_2 = \frac{1}{2} \det \begin{bmatrix} 1 & 1 & 1 \\ x_1 & x_3 & x_4 \\ y_1 & y_3 & y_4 \end{bmatrix},$$

$$T_3 = \frac{1}{2} \det \begin{bmatrix} 1 & 1 & 1 \\ x_1 & x_2 & x_4 \\ y_1 & y_2 & y_4 \end{bmatrix}, \quad T_4 = \frac{1}{2} \det \begin{bmatrix} 1 & 1 & 1 \\ x_1 & x_2 & x_3 \\ y_1 & y_2 & y_3 \end{bmatrix}.$$

Now, let us consider the coefficient matrix of the linear system in (14). Carrying out the expansion with respect to the last row, it can be directly verified that its determinant is equal to $2|Q|$. By directly solving system (14) through Cramer's rule, and expanding the determinant with respect to the i -th column, we obtain

$$\varphi_i = (a_i + b_i x + c_i y) + (-1)^i \frac{T_i}{|Q|} \Psi_h, \quad i = 1, \dots, 4,$$

where

$$a_i = \frac{(-1)^i T_i + (x_{i+1} y_{i-1} - x_{i-1} y_{i+1})}{2Q},$$

$$b_i = \frac{y_{i+1} - y_{i-1}}{2|Q|} = \frac{(i)_y}{2|Q|}, \quad c_i = -\frac{x_{i+1} - x_{i-1}}{2|Q|} = -\frac{(i)_x}{2|Q|}.$$

We conclude that

$$\varphi_i(\mathbf{x}) = a_i + \frac{\mathbf{d}_i^\perp}{2|Q|} \cdot \mathbf{x} + (-1)^i \frac{T_i}{|Q|} \Psi_h(\mathbf{x}).$$

On defining the non-dimensional quantities

$$T'_i := (-1)^i \frac{T_i}{|Q|},$$

we have

$$\varphi_i(\mathbf{x}) = a_i + \frac{\mathbf{d}_i^\perp}{2|Q|} \cdot \mathbf{x} + T'_i \Psi_h(\mathbf{x}).$$

Hence we have the following identities:

$$(\mathbf{I} - \Pi_1^\nabla)\varphi_i = T_i' \Psi_h, \quad (15)$$

and

$$(\mathbf{I} - \Pi_0^0)\nabla\varphi_i = \nabla\varphi_i - \nabla\Pi_1^\nabla\varphi_i = \nabla(\varphi_i - \Pi_1^\nabla\varphi_i) = T_i' \nabla\Psi_h. \quad (16)$$

The second term of (5) can then be written as

$$\int_Q \kappa(\mathbf{I} - \Pi_0^0)\nabla\varphi_j \cdot (\mathbf{I} - \Pi_0^0)\nabla\varphi_i \, d\mathbf{x} = T_i' T_j' \int_Q \kappa \nabla\Psi_h \cdot \nabla\Psi_h \, d\mathbf{x}$$

and the matrix \mathbf{B} of (2) is identified by

$$\mathbf{B}_{ij} = T_i' T_j'.$$

Setting $\gamma := [T_1' \ T_2' \ T_3' \ T_4']'$, the matrix \mathbf{B} can be written as $\mathbf{B} = \gamma\gamma^\mathbf{T}$. Note that if Q is a parallelogram, we have

$$T_i' = (-1)^i \frac{1}{2}$$

so that \mathbf{B} is independent on Q :

$$\mathbf{B} = \frac{1}{4} \begin{bmatrix} +1 & -1 & +1 & -1 \\ -1 & +1 & -1 & +1 \\ +1 & -1 & +1 & -1 \\ -1 & +1 & -1 & +1 \end{bmatrix}.$$

We end up with the formula:

$$\int_Q \kappa \nabla\varphi_j \cdot \nabla\varphi_i \, d\mathbf{x} = \frac{1}{4|Q|} \kappa \mathbf{d}_j^\perp \cdot \mathbf{d}_i^\perp + \left[\int_Q \kappa \nabla\Psi_h \cdot \nabla\Psi_h \, d\mathbf{x} \right] \gamma\gamma^\mathbf{T} = \mathbf{A} + \tau\mathbf{B}.$$

Clearly, the only term that depends on the variation of the generalized barycentric coordinates inside Q is the coefficient

$$\tau = \int_Q \kappa \nabla\Psi_h \cdot \nabla\Psi_h \, d\mathbf{x},$$

which is the *energy of the hourglass mode* Ψ_h .

3 Value of τ for some GBCs

For a general quadrilateral usually the value of τ does not have an expression in closed form. In this Section, we report the value of τ for isoparametric finite element shape functions and Wachspress coordinates over rectangles and parallelograms.

3.1 Rectangles

For a rectangle, isoparametric FEM, harmonic generalized barycentric coordinates [10] and Wachspress shape functions coincide. If $Q = [0, a] \times [0, b]$, the value of τ for a general κ is given by

$$\tau = \frac{b^2 \kappa_{11} + a^2 \kappa_{22}}{3ab}. \quad (17)$$

3.2 Parallelograms

For a parallelogram, isoparametric FEM and Wachspress GBCs coincide. In this case, the value of τ is given by:

- When $\kappa = \kappa \mathbf{I}$, and Q is a parallelogram of sides a and b with angle θ :

$$\tau = \kappa \frac{a^2 + b^2}{3ab \sin \theta}.$$

- For general κ , and if Q is a parallelogram of sides a and b with angle θ , with side a parallel to the x -axis:

$$\tau = \frac{a^2 \kappa_{22} + b^2 \kappa_{11}}{3ab \sin \theta} + \frac{b \left((\kappa_{22} - \kappa_{11}) \cos^2 \theta - 2 \kappa_{12} \cos \theta \sin \theta \right)}{3a \sin \theta}.$$

4 Connection with Virtual Element Method

The virtual element method is a fairly recent methodology that in particular extends classical finite elements to polygonal and polyhedral meshes, see [11] and the references therein. The keys ideas in VEM are:

- the local space is ‘virtual’ in the sense that functions are known only through their degrees of freedom;
- the element stiffness matrix is split into a ‘consistency’ term that takes care of the accuracy plus a ‘stability’ term that ensures stability without violating consistency:

$$\mathbf{K}_{\text{VEM}} = \mathbf{K}_{\text{C}} + \mathbf{K}_{\text{S}}.$$

4.1 Linear virtual element on a polygon

In the case of linear virtual elements for the diffusion equation, the ‘basic’ local space coincides with harmonic GBCs, whereas the ‘enhanced’ version [2] is still a GBC, but the local functions are no longer harmonic. The consistency and stability matrices in the VEM are built upon the construction of the Π_1^{∇} projection, which can be extended to a general polygon P with N_P vertices by following the above construction, and is still given by (11) (see [1,2,12] for the details).

In the case $\boldsymbol{\kappa}$ is a constant matrix, for the diffusion problem the local VEM consistency matrix \mathbf{K}_C coincides with the matrix \mathbf{A} of the decomposition (2):

$$(\mathbf{K}_C)_{ij} = \mathbf{A}_{ij} = \int_P \boldsymbol{\kappa} \Pi_0^0 \nabla \varphi_j \cdot \Pi_0^0 \nabla \varphi_j \, d\mathbf{x} = \int_P \boldsymbol{\kappa} \nabla \Pi_1^\nabla \varphi_j \cdot \nabla \Pi_1^\nabla \varphi_j \, d\mathbf{x} = \frac{1}{4|P|} \boldsymbol{\kappa} \mathbf{d}_j^\perp \cdot \mathbf{d}_i^\perp.$$

The VEM stability matrix \mathbf{K}_S for a polygon P is built in the following way. Let \mathcal{S} be a symmetric bilinear form defined on the local space that ‘scales’ on the kernel of Π_1^∇ like the bilinear form associated with the differential equation, i.e., there exist two constants α_* and α^* independent of the element P such that

$$\alpha_* \int_P \boldsymbol{\kappa} \nabla v_h \cdot \nabla v_h \, d\mathbf{x} \leq \mathcal{S}(v_h, v_h) \leq \alpha^* \int_P \boldsymbol{\kappa} \nabla v_h \cdot \nabla v_h \, d\mathbf{x} \quad \text{for all } v_h \in \ker \Pi_1^\nabla.$$

Then if we define

$$(\mathbf{K}_S)_{ij} := \mathcal{S}((\mathbf{I} - \Pi_1^\nabla)\varphi_j, (\mathbf{I} - \Pi_1^\nabla)\varphi_i), \quad (18)$$

we have a convergent method (see Theorem 3.1 and 4.1 of [1]).

In order to construct a computable \mathcal{S} satisfying the hypotheses above, we proceed in the following way. Define $\text{dof}_i(v_h)$ as the i -th degree of freedom of v_h in the linear case, that is

$$\text{dof}_i(v_h) := v_h(V_i), \quad i = 1, \dots, N_P$$

and then set

$$\mathcal{S}(u_h, v_h) := \tau_{\text{VEM}} \sum_{i=1}^{N_P} \text{dof}_i(u_h) \text{dof}_i(v_h) \quad (\text{dof-dof stabilization})$$

where τ_{VEM} is a parameter to be fixed (see Section 4.2 of [13]). Under reasonable assumptions on the mesh sequence (quadrilaterals are not degenerate) to have convergence when the mesh size goes to zero, we can take any non-zero constant for τ_{VEM} , provided that all τ_{VEM} ’s for all polygons and for all meshes are uniformly bounded from below and above. In other words, we can say that τ_{VEM} *must scale like 1*. If we are in three dimensions we require that τ_{VEM} *scales like h*.

Hence, the final expression for the local stability \mathbf{K}_S is the following:

$$(\mathbf{K}_S)_{ij} = \tau_{\text{VEM}} \sum_{k=1}^{N_P} \text{dof}_k[(\mathbf{I} - \Pi_1^\nabla)\varphi_j] \text{dof}_k[(\mathbf{I} - \Pi_1^\nabla)\varphi_i].$$

In the next section, we examine a practical choice for τ_{VEM} .

4.2 Revisiting quadrilaterals

From now on we consider a polygon to be a quadrilateral Q . In this case, we have

$$\sum_{k=1}^4 \text{dof}_k[(\mathbf{I} - \Pi_1^\nabla)\varphi_j] \text{dof}_k[(\mathbf{I} - \Pi_1^\nabla)\varphi_i] = \mathbf{B}_{ij},$$

where \mathbf{B} is the matrix appearing in the decomposition (2). In fact, since $(\mathbf{I} - \Pi_1^\nabla)\varphi_i = T'_i \Psi_h$ (see (15)) and $\Psi_h = \frac{1}{2} \sum_{\ell=1}^4 (-1)^\ell \varphi_\ell$, we have

$$\text{dof}_k[(\mathbf{I} - \Pi_1^\nabla)\varphi_i] = T'_i \sum_{\ell=1}^4 \frac{(-1)^\ell}{2} \text{dof}_k(\varphi_\ell) = T'_i \sum_{\ell=1}^4 \frac{(-1)^\ell}{2} \delta_{k\ell} = T'_i \frac{(-1)^k}{2}$$

so that

$$\sum_{k=1}^4 \text{dof}_k[(\mathbf{I} - \Pi_1^\nabla)\varphi_j] \text{dof}_k[(\mathbf{I} - \Pi_1^\nabla)\varphi_i] = T'_j T'_i \sum_{k=1}^4 \left[\frac{(-1)^k}{2} \right]^2 = T'_j T'_i = \mathbf{B}_{ij}.$$

To summarize, the element VEM stiffness matrix for a quadrilateral can be written as

$$\mathbf{K}_{\text{VEM}} = \mathbf{A} + \tau_{\text{VEM}} \mathbf{B}. \quad (19)$$

5 How to choose τ_{VEM} ?

The decompositions in (2) and in (19) for GBCs and VEM, respectively are:

$$\mathbf{K} = \mathbf{A} + \tau \mathbf{B} \quad \text{and} \quad \mathbf{K}_{\text{VEM}} = \mathbf{A} + \tau_{\text{VEM}} \mathbf{B},$$

which are formally equal, but very different in practice.

- In the case of GBCs, the value of the parameter τ is well defined as the energy of a particular function (the hourglass mode Ψ_h) of the local space:

$$\tau = \int_Q \boldsymbol{\kappa} \nabla \Psi_h \cdot \nabla \Psi_h \, d\mathbf{x}.$$

The value of τ can be computed by quadrature; actually, computing τ by a quadrature formula and using the decomposition (2) is equivalent to approximating directly \mathbf{K} (as defined in (1)) with the same quadrature formula.

- For VEM, the parameter τ_{VEM} is left unspecified, and we only require that convergence hypotheses are satisfied. In this very particular case (quadrilaterals, linear VEM, $\boldsymbol{\kappa}$ constant) the value of τ_{VEM} could be in principle identified with the energy of the corresponding hourglass mode of the VEM space, but the extremely wide range of applicability of VEM (general polygons and polyhedra, polynomials of any order, elasticity, Navier–Stokes, magnetostatics problems) prevents in most instances a constructive approach for the computation of τ_{VEM} .

Here we will use the interpretation of the ‘correct’ τ_{VEM} as the energy of the hourglass mode Ψ_h to draw some general conclusions about the design of τ_{VEM} and the consequences of having employed an ‘incorrect’ τ_{VEM} .

First of all, it seems natural to include in τ_{VEM} some information from $\boldsymbol{\kappa}$. This is not needed for convergence, but for a given mesh if $\boldsymbol{\kappa}$ is large we could have a marked difference in the solution. We then set:

$$\tau_{\text{VEM}} = \frac{\text{tr } \boldsymbol{\kappa}}{2}. \quad (20)$$

Hence, regardless of the shape of the quadrilateral Q and of the local VEM space, in the VEM the energy of the hourglass mode Ψ_h is always set to $\text{tr } \boldsymbol{\kappa}/2$.

As observed in many papers on VEM, the sensitivity with respect to the value of τ_{VEM} is usually mild: the value in (20) works well for a wide range of polygonal shapes. We now provide explanation and clarification for this observation.

5.1 The worst case for VEM

The worst scenario for VEM on a given mesh is the following:

- the value of τ_{VEM} is a bad approximation of the energy of Ψ_h ;
- the exact solution of the PDE ‘contains’ the hourglass mode Ψ_h .

Note, however, that the hourglass mode Ψ_h depends on the mesh; hence upon refinement we are led to a ‘better’ solution.

5.2 Effect of τ_{VEM} in a Laplace problem

Consider the following Laplace problem with inhomogeneous Dirichlet boundary conditions:

$$\begin{cases} -\Delta u = 0 & \text{in } \Omega = (0,1)^2, \\ u = g & \text{on } \partial\Omega, \end{cases} \quad (21)$$

where g is a continuous, piecewise linear function that oscillates 20 times on each edge from $-1/4$ to $+1/4$. The exact solution u decays very quickly to zero inside the domain; see the reference solution shown in Fig. 3.

Now we want to use a mesh such that the hourglass mode Ψ_h has a strong component in the exact solution u . We divide Ω into 20×20 uniform squares, in such a way that the boundary condition g oscillates precisely as Ψ_h . Hence, if the numerical scheme does not adopt the correct value of the energy of Ψ_h , it will propagate g inside the domain and lead to an incorrect solution. This is similar to hourglass modes in a FEM mesh that can become communicable and wreck the solution [9]. In the first experiment we consider isoparametric FEM (see Fig. 4a) and VEM with $\tau_{\text{VEM}} = 1$ (see Fig. 4b). Given that the mesh is coarse, the numerical solutions are adequate; however, note that the two solutions are distinct.

Remark 4. From (20), $\tau_{\text{VEM}} = \text{tr } \boldsymbol{\kappa}/2$; here $\boldsymbol{\kappa} = \mathbf{I}$, so $\tau_{\text{VEM}} = 1$. On a square, VEM with $\tau_{\text{VEM}} = 2/3$ is identical to isoparametric FEM (see (17)).

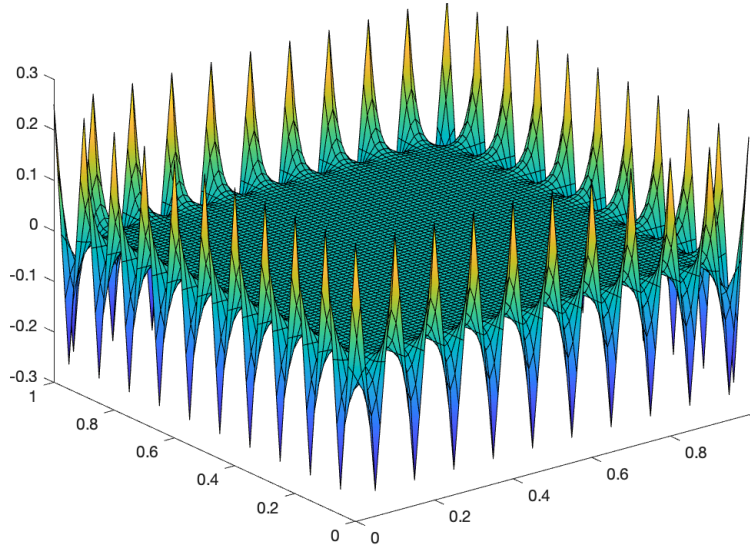


Fig. 3: Reference finite element solution to the problem posed in (21).

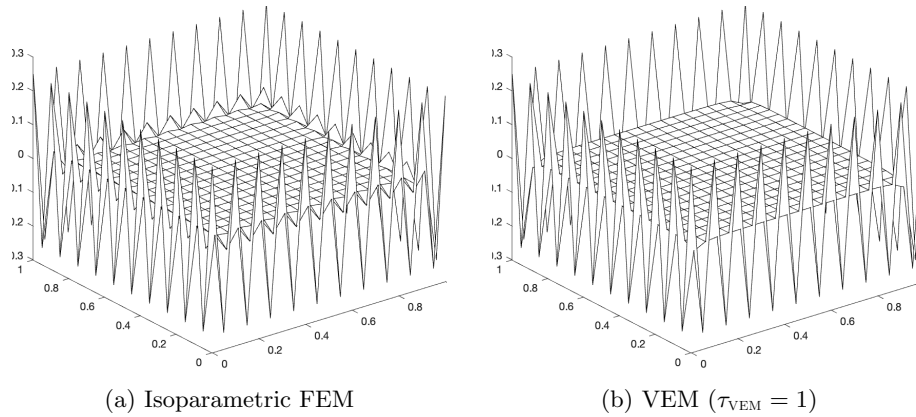


Fig. 4: Numerical solution for isoparametric FEM and VEM on a 20×20 mesh.

Now we take VEM with $\tau_{\text{VEM}} = 0.1$, and we can see that the virtual element solution worsens (see Fig. 5a). If we further decrease the value of τ_{VEM} to 0.01, then the boundary data g is almost free to move in the domain since dissipation is very small (Fig. 5b). The numerical solution is also unstable for $\tau_{\text{VEM}} = 10$ and $\tau_{\text{VEM}} = 100$, as is observed in Figs. 5c and 5d.

However, if we refine and consider a 40×40 mesh of uniform squares, the two values 0.1 and 10 for τ_{VEM} become acceptable, as is seen in Figs. 6a and 6b. The reason for this observation is that now the hourglass mode Ψ_h has a smaller component in the exact solution u , and even if its energy of Ψ_h is not precise, its

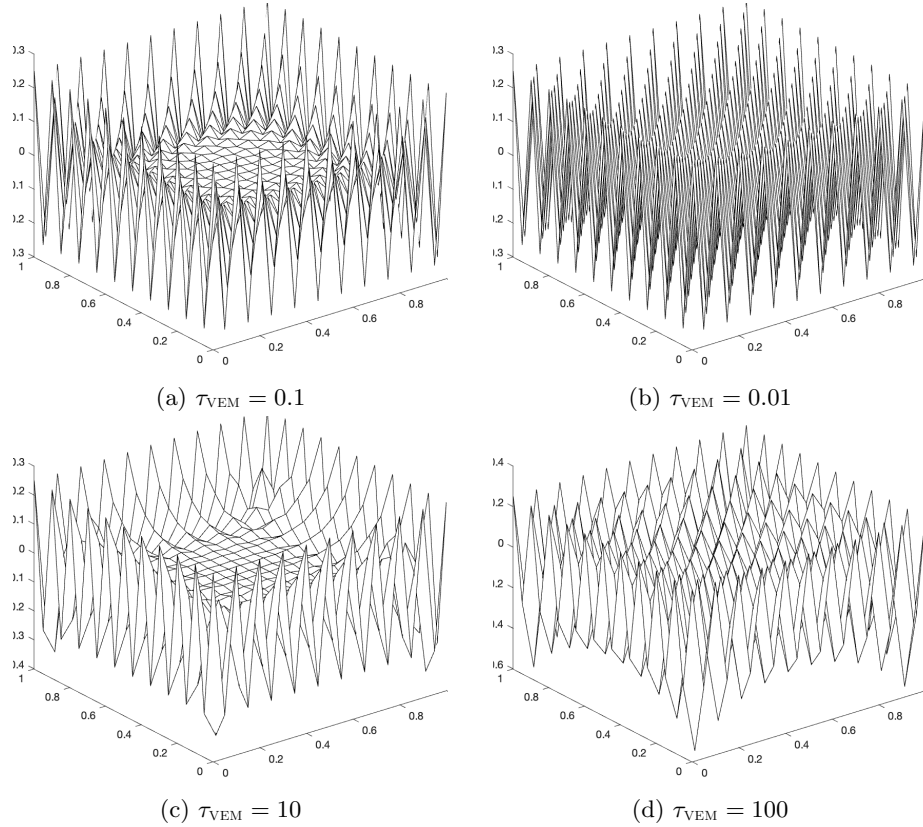


Fig. 5: Numerical solution using different τ_{VEM} for the VEM on a 20×20 mesh.

impact on the numerical solution is not severe. As the mesh is further refined, the virtual element solution becomes more and more insensitive to τ_{VEM} , as shown in Figs. 7a–7d.

5.3 Numerical comparison between isoparametric FEM and VEM

Consider the following diffusion problem in the unit square, $\Omega = (0, 1)^2$:

$$\begin{cases} -\operatorname{div}(\boldsymbol{\kappa}\nabla u) = f & \text{in } \Omega \\ u = g & \text{on } \partial\Omega \end{cases} \quad (22)$$

where $\boldsymbol{\kappa}(x, y) = \begin{bmatrix} 1 + y^2 & -xy \\ -xy & 1 + x^2 \end{bmatrix}$ and f and g are chosen in such a way that

$$u(x, y) = x^3 - xy^2 + x^2y - xy + x^2 - x + y - 1 + \sin(5x)\sin(7y) + \log(1 + x^2 + y^4)$$

is the exact solution. In each element, $\boldsymbol{\kappa}$ is approximated with its value at the barycenter of the element. We compare isoparametric FEM and VEM on two

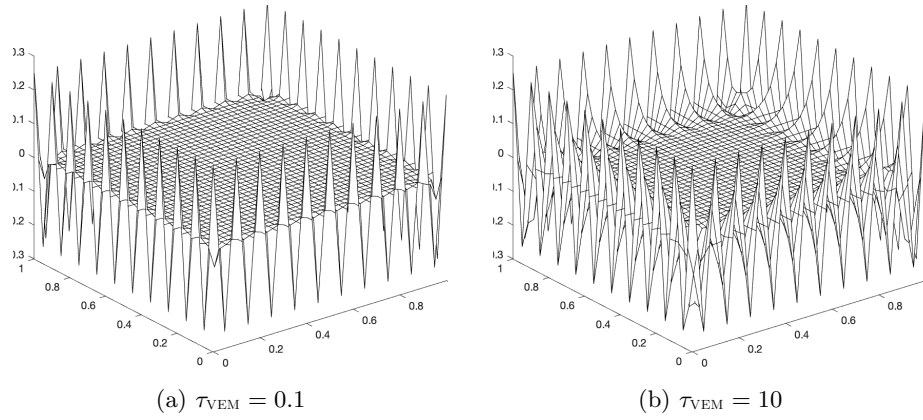


Fig. 6: Numerical solution using different τ_{VEM} for the VEM on a 40×40 mesh.

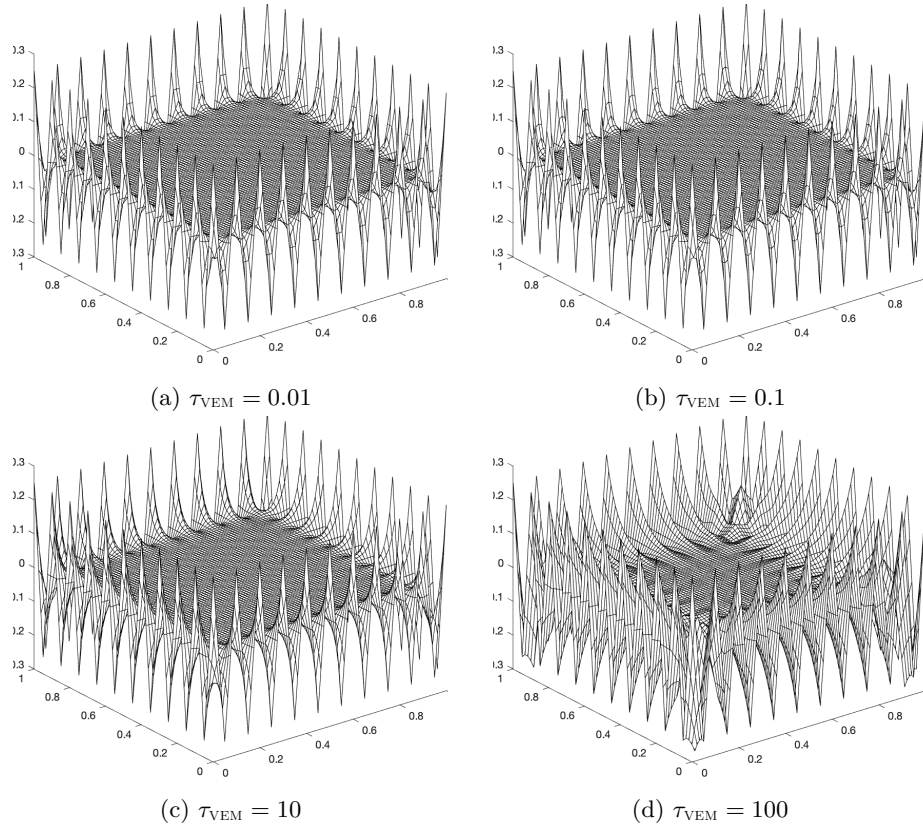


Fig. 7: Numerical solution using different τ_{VEM} for the VEM on a 80×80 mesh.

meshes of irregular quadrilaterals that are shown in Fig. 8. The numerical results on the two meshes are presented in Figs. 9 and 10. We observe that the solutions of FEM and VEM are indistinguishable with proximal errors in the L_∞ norm.

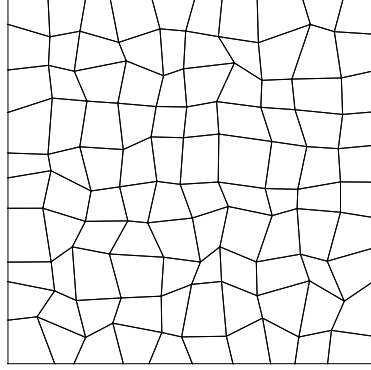
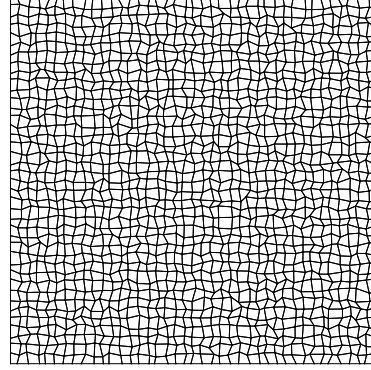
(a) 10×10 mesh; $h_{\text{mean}} = 0.16$ (b) 40×40 mesh; $h_{\text{mean}} = 0.04$

Fig. 8: Finite element meshes used in the FEM and VEM to solve (22).

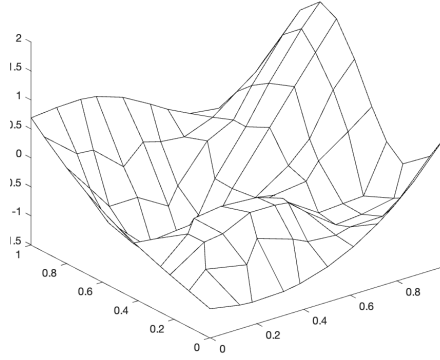
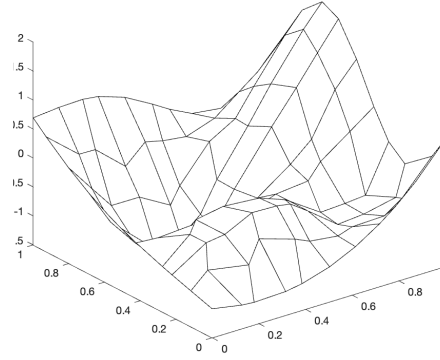
(a) FEM, $|u - u^h|_\infty = 3.6 \times 10^{-2}$ (b) VEM, $|u - u^h|_\infty = 2.4 \times 10^{-2}$

Fig. 9: Error at vertices for isoparametric FEM and VEM on the mesh shown in Fig. 8a.

6 Conclusions

Our main conclusion from this study is that VEM is relatively insensitive with respect to the stabilization parameter τ_{VEM} . A caveat in reaching this inference

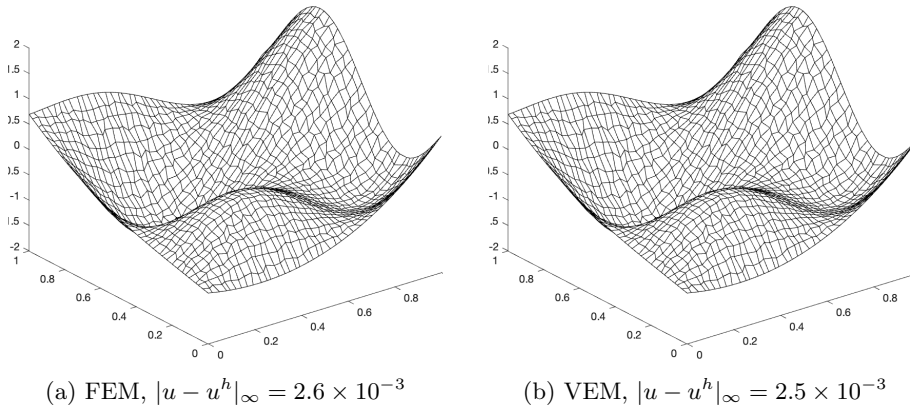


Fig. 10: Error at vertices for isoparametric FEM and VEM on the mesh shown in Fig. 8b.

is that the mesh must be fine enough so that the hourglass modes are no longer present in the exact solution. As we have shown in the numerical experiment, coarse mesh accuracy and stability can be compromised if the hourglass function is a Dirichlet boundary condition that is exactly imposed. As part of future work, we plan to extend our analysis to distorted quadrilaterals, and to also include mean value coordinates and harmonic coordinates in our study.

References

1. L. Beirão da Veiga, F. Brezzi, A. Cangiani, G. Manzini, L. D. Marini, A. Russo: Basic principles of Virtual Element Methods. *Math. Models Methods Appl. Sci.* 23 (2013), 199–214.
2. B. Ahmad, A. Alsaedi, F. Brezzi, L. D. Marini, A. Russo: Equivalent projectors for virtual element methods, *Comput. Math. Appl.* 66(3) (2013), 376–391
3. K. Hormann, N. Sukumar: *Generalized Barycentric Coordinates in Computer Graphics and Computational Mechanics*, Boca Raton: Taylor & Francis, CRC Press, 2017.
4. E. L. Wachspress: *Rational Bases and Generalized Barycentric*, Cham: Springer, 2016
5. M. S. Floater: Mean value coordinates, *Comput. Aided Geom. Des.* 20(1) (2003), 19–27.
6. M. S. Floater: Generalized barycentric coordinates and applications *Acta Numerica* 24 (2015), 161–214.
7. A. Cangiani, G. Manzini, A. Russo, N. Sukumar: Hourglass stabilization and the virtual element method, *Int. J. Numer. Methods Eng.* 102(3–4) (2015), 404–436.
8. D. P. Flanagan, T. Belytschko: A uniform strain hexahedron and quadrilateral with orthogonal hourglass control, *Int. J. Numer. Methods Eng.* 17(5) (1981), 670–706.
9. T. Belytschko, W. K. Liu, B. Moran, K. Elkhodary: *Nonlinear Finite Elements for Continua and Structures*, John Wiley & Sons, Second Edition, 2014.

10. P. Joshi, M. Meyer, T. DeRose, B. Green, T. Sanocki: Harmonic coordinates for character articulation, *ACM Trans. Graph.* 26(3) (2007), Article 71, 9 pages
11. L. Beirão da Veiga, F. Brezzi, L. D. Marini, A. Russo: The Virtual Element Method, *Acta Numerica* 32 (2023), doi:10.1017/S0962492922000095.
12. L. Beirão da Veiga, F. Brezzi, L. D. Marini, A. Russo: The hitchhiker guide to the Virtual Element Method, *Math. Models Methods Appl. Sci.* 24 (2014), 1541–1573.
13. L. Beirão da Veiga, F. Brezzi, L. D. Marini, A. Russo: Virtual Element Methods for general second order elliptic problems on polygonal meshes, *Math. Models Methods Appl. Sci.* 26 (2014), 729–750.